Nuclear Magnetic Resonance Gyroscopes

E. A. Donley
Time and Frequency Division
National Institute of Standards and Technology
325 Broadway, Boulder, CO 80305
edonley@boulder.nist.gov

***Abstract*— Nuclear magnetic resonance gyroscopes (NMRGs) detect rotation as a shift in the Larmor precession frequency of nuclear spins. A review of the open literature on NMRGs is presented, which includes an introduction to the spectroscopic techniques that enable NMRGs and a discussion of the design details for several specific NMRGs that have been built.**

I. INTRODUCTION

A gyroscope measures the angle or angular rate of rotation of the object upon which it is mounted relative to inertial space. Nuclear magnetic resonance gyroscopes (NMRGs) accomplish rotation detection by measuring a shift in the Larmor precession frequency of nuclear spins in an applied magnetic field. Large-scale NMRGs were developed in the 1960s and 70s, with both Singer and Litton producing optically pumped NMRGs with bias drifts lower than 0.1 °/h [1]. Prior to this review article, several other reviews of this early work had been published. The reviews by Karwacki and Woodman et al. present detailed specific approaches to NMRGs [2], [3]. The article by Kuritsky et al. provides a review of inertial navigation that includes NMRG work performed through 1983 [4]. The recent review by Liu et al. presents recent developments in the field of microfabricated gyroscopes and includes some discussion of NMRGs [5].

Here I attempt to tie together developments in NMRGs that have occurred over the past 50 years including recent miniaturization trends. Section II gives an introduction into the instrumentation and measurement techniques for NMRGs. Following that, specific examples of NMRGs are given, including those based on mercury (section III) and on noble gases (section IV). In section V, studies on nuclear quadrupolar effects are presented, which cause shifts and splittings in NMRG spectra. Section VI gives a review of the comagnetometer approach, which has recently been used to demonstrate a high-performance NMRG. In section VII, developments in miniaturization are presented. Apologies are given to groups that are not sufficiently credited due to space limitations or unintentional omissions.

The views, opinions, and/or findings contained in this article/presentation are those of the author/presenter and should not be interpreted as representing the official views or policies, either expressed or implied, of the Defense Advanced Research Projects Agency or the Department of Defense.

(Approved for Public Release, Distribution Unlimited)

II. TECHNICAL BACKGROUND

A simplified version of a typical NMR gyroscope is presented in Fig. 1. A vapor cell contains one or more active NMR isotopes such as ^{129}Xe, an alkali atom such as ^{87}Rb, and some buffer gas. A circularly polarized pump beam resonant with an optical transition in the Rb atoms and oriented parallel to an applied field B_0 spin polarizes the Rb atoms. The Rb polarization is transferred to the Xe nuclei through collisions, thereby creating a macroscopic spin polarization for both species. Coherent spin precession is generated for both species with applied AC magnetic fields (not shown) perpendicular to B_0. The Xe spins precess about the direction B_0, with a precession frequency proportional to the magnitude of the applied field, $\omega_{Xe} = \gamma_{Xe} B_0$. The proportionality constant is the gyromagnetic ratio, γ_{Xe}, which depends on the properties of the nucleus and is equal to the ratio of its nuclear magnetic dipole moment to its angular momentum.

The Rb spins precess about the total field, which is the sum of B_0 and the field generated by the precessing Xe spins.

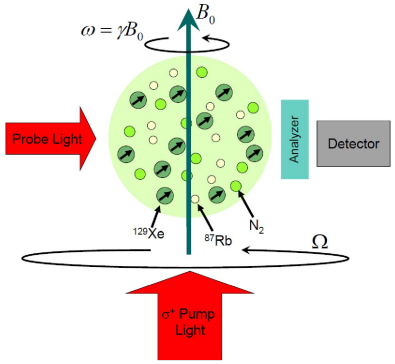

Figure 1. The basic elements of an NMR gyroscope. For a discussion of the various components, see the text.

The Rb polarization is monitored with a probe beam, and from this signal, the orientation of the Xe polarization can be detected. This is done either by observing modulation of the optical absorption of a circularly polarized probe or by observing rotation of the plane of polarization of a linearly polarized probe, by use of a polarization analyzer. (The magnetometry techniques are discussed in detail below.)

When the gyroscope apparatus is rotating about the axis of the applied field B_0 at a frequency Ω, the measured Larmor precession frequency is

$$\omega_{\mathrm{Xe}} = \gamma_{\mathrm{Xe}} B_0 \pm \Omega . \qquad (1)$$

Ω is the rotation rate of the apparatus, or more specifically, the rotation rate of the probe beam and drive fields (the observer) with respect to inertial space. The sign of the shift depends on the direction of rotation. In effect, the observer is fixed to the apparatus and the nuclei are free to precess in the magnetic field untethered to the cell walls.

A productive period of research in the early 1960's solved several technical problems that improved NMRG feasibility, including magnetic field stabilization, polarization enhancement through optical pumping and spin-exchange optical pumping, and optical detection. These techniques are presented in detail below.

A. Magnetic-Field Control

To determine Ω, B_0 needs to be stable and precisely known. Given the gyromagnetic ratio for ^{129}Xe of $2\pi \cdot 10$ MHz/T, a 1°/h bias instability corresponds to a field instability of 100 fT (one billionth the size of the earth's magnetic field). The ambient earth field (which is not necessarily constant) can typically be reduced only by a factor of 10^7 by use of magnetic shields [6], [7].

Early in NMRG development, a two-isotope solution was found to stabilize the field [8]. Two NMR isotopes contained in an NMRG vapor cell will have the precession frequencies

$$\omega_1 = \gamma_1 B_0 \pm \Omega ,$$
$$\omega_2 = \gamma_2 B_0 \pm \Omega . \qquad (2)$$

Isotopes 1 and 2 have different magnetic-field shifts owing to their different values of γ, but they have the same rotational shifts. Since there are two simultaneous equations and two unknowns (B_0 and Ω), the field dependence can be removed by simultaneously monitoring both precession frequencies.

B. Optical Pumping

In the earliest proposals for NMRGs, the probed nuclei were in thermal equilibrium, and the net polarization of the sample was very low [9], [10], [11]. Owing to Boltzmann statistics, in thermal equilibrium, the $|-1/2\rangle$ state has a population that is only very slightly higher than the population of the $|+1/2\rangle$ state, and the system has a low degree of polarization. The polarization is defined as the normalized population difference between the two ground states. Since the sample magnetization is proportional to the polarization, a low polarization leads to weak NMR signals.

In 1950 Kastler pointed out that the absorption and scattering of circularly polarized light could lead to large population imbalances in the ground states and high degrees of atomic polarization [12]. A basic description of this "optical pumping" technique is shown in Fig. 2. For a detailed review of optical pumping, see [13].

Optical pumping can enhance the sample polarization for a typical sample of alkali atoms from a very small fraction of a percent to nearly 100 %, depending on the sample relaxation mechanisms. Early versions of gyroscopes based on electron paramagnetic resonance adopted the technique [14], [15]. Simpson et al. also used optical pumping to enhance the nuclear spin-polarization of mercury for NMRGs [8]. Details on Hg NMRGs are presented in Section III, below. Hg has a $^1S_0$ ground state and no net unpaired electrons; thus the picture of optical pumping presented in Fig. 2 does not strictly apply, but the nuclear spin for Hg atoms can be optically pumped directly with a Hg lamp. Happer's optical pumping review [13] presents the physics of the optical pumping of Hg in detail.

C. Spin-exchange optical pumping

Spin-exchange optical pumping (SEOP) on mixtures of alkali and noble-gas atoms can be used to efficiently polarize noble-gas nuclei. During the SEOP process, the electronic spin polarization of the alkali atoms is transferred to the noble-gas nuclei through collisions. Bouchiat et al. were the first to demonstrate this effect [16], where they observed a spin-polarization for ^{3}He of 1%, which is enhanced by a factor of 10,000 from the Boltzmann determined polarization of 10^{-8}. NMRGs based on noble-gas nuclei use the technique to generate spin-polarized noble-gas samples [17].

Today, SEOP is routinely used to generate spin-polarized samples of noble-gas nuclei with polarizations of many tens of percent. For a modern review of spin-exchange optical pumping, see the review by Walker and Happer [18].

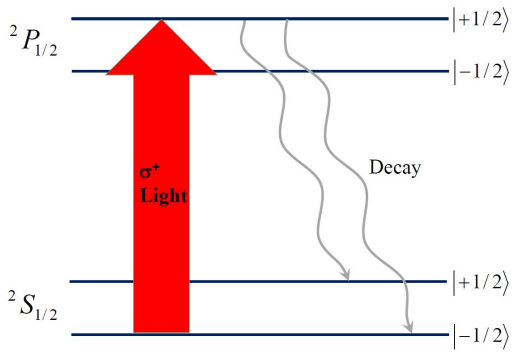

Figure 2. Optical pumping for an alkali atom with electronic $^2S_{1/2}$ and $^2P_{1/2}$ states. These states are each split into two sublevels according to the relative alignment of the electron and nuclear spins, with the higher-energy, higher-momentum state, $|+1/2\rangle$, corresponding to the two spins oriented along the same direction. (Any additional splittings and shifts from applied magnetic fields are not shown.) Under illumination with circularly polarized light, only excitation from the $|-1/2\rangle$ to the $|+1/2\rangle$ sublevels is allowed, since the photons also carry angular momentum. Since an atom in the $|+1/2\rangle$ excited state can decay to either ground state through radiative decay or quenching, ignoring relaxation, all of the atoms will eventually be pumped into the $|+1/2\rangle$ ground-state sublevel.

D. Magnetometry Techniques for Optical Detection

1) The Dehmelt Technique

The same physics that enables optical pumping can also be used for detection of the spin precession, which was first pointed out by Dehmelt [19]. The absorption of a circularly polarized probe beam depends on the projection of the atomic spin along the direction of propagation of the probe. When the spin vector (and hence the magnetization) is aligned with the probe, the absorption is minimized (the atoms are already optically pumped). When the spin vector points in the opposite direction, the absorption is a maximum. If the magnetization makes an angle θ with respect to the field and precesses at a frequency ω about the z axis and the probe beam propagates in the x direction, the fraction of the atoms in the absorbing state will be $f = (1 - \sin\theta\cos\omega t)/2$. Thus, ω can be detected as modulations of the probe-beam absorption. Since the pump and probe beams both have the same polarization, they can originate from the same beam that is propagating at some angle between the light propagation direction and the magnetic field as shown in Fig. 3. Litton used this approach [17], discussed below in section IV.

2) Faraday Rotation Detection

Spin precession can also be monitored by measuring the rotation of the plane of polarization of a linearly polarized probe beam caused by the Faraday effect. (For a review of the Faraday effect, see [20] and the references therein.) For linearly polarized light passing through a magneto-optical system with a magnetic field oriented along the direction of light propagation, the left- and right-circularly polarized components of the light beam acquire different phase shifts, which results in a rotation of the plane of polarization that can be observed with a polarizer and a detector. The probe beam frequency can be detuned from resonance such that the absorption of the probe is low.

E. Excitation of a coherent spin precession

Weak excitation fields are applied to the sample to drive resonant coherent spin precession for both nuclear isotopes as well as any alkali-atom isotope that is used for spin-exchange optical pumping and detection. A schematic drawing of one of the many possible configurations for driving the spins and measuring the precession frequencies is shown in Fig. 3. In this example, a vapor cell containing ^{129}Xe, Rb, and some buffer gas is located at the origin of the coordinate axes. A magnetic field B_0 is applied in the x – z plane, and a single circularly polarized laser beam that serves both for optical pumping and detection propagates along the x direction.

The Xe spins are made to precess in phase about B_0 by the AC field ΔB_{Xe} applied along the x direction. The Xe magnetization generates a magnetic field, and the total field as sensed by the Rb atoms also precesses about the direction of B_0. Because the gyromagnetic ratios for alkali spins are about 1000× larger than the gyromagnetic ratios for the noble-gas nuclear spins, the precessing magnetic field is slow compared to the Rb Larmor frequency, and the Rb precesses about the total field B_T. The Rb spin precession is driven with an applied AC magnetic field, ΔB_{Rb}. The light reaching the photodiode is intensity-modulated at the Rb precession frequency with a superimposed AM modulation at the Xe precession frequency. The individual signals are extracted via two lock-in amplifiers (three lock-in amplifiers if two noble-gas isotopes are used). The out-of-phase lock-in signal has the desirable property that it is nearly linear, and passes through zero, near the resonance. If the excitation frequency is fixed near the resonance, the calibrated slope from the dispersion signal can be used to determine changes in the nuclear precession rate. When two nuclear isotopes are used, field stabilization/cancellation as described above can be achieved.

III. NMRGs Based on Spin-Polarized Mercury

Starting in the early 1960's, there was a significant amount of work performed on NMRGs. Singer's approach was based on the mercury isotopes ^{199}Hg and ^{201}Hg [8], [21]. As of 1980, they achieved a reported value of 0.053 °/√h for the angle random walk (ARW) [2]. Details on their approach are given in [22] and [23] and reviewed in [4]. In addition to interrogating two NMR isotopes for magnetic field control, they also used two vapor cells containing both nuclei that were placed in oppositely-directed magnetic fields to remove the requirement of precisely knowing the gyromagnetic ratios of the NMR isotopes.

The Hg nuclear spins were pumped directly and probed via a ^{204}Hg lamp at 253.7 nm. The nuclei were probed via Faraday rotation. The system of two cells in oppositely directed equal fields gives a simple determination of the rotation rate, $\Omega = (\omega_1 + \omega_2 - \omega_1^* - \omega_2^*)/4$, where the stars indicate the frequencies measured in the second cell. The magnitudes of the oppositely oriented magnetic fields can be held constant by use of the difference frequencies between the two isotopes in each cell to generate an error signal for the field. A detailed noise analysis for their experiments is presented in [24], and a similar approach based on one cell was proposed by Karwacki and Griffin [25].

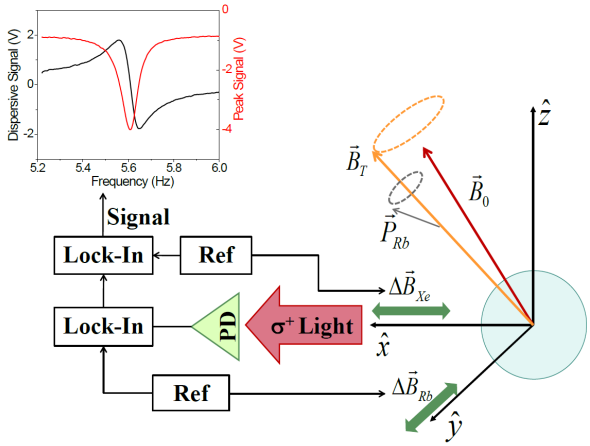

Figure 3. Spin precession excitation scheme (see text). The graph is a Xe magnetic resonance measured in our laboratory, with the x axis representing the ^{129}Xe excitation frequency and the y axes showing the lock-in signals. Here the magnetic field was about 0.5 μT. This example is one of many pump/probe/field geometries that works for detecting the Xe spin precession frequency.

IV. NMRGs Based on Noble-Gas Nuclei

Beginning in the late 1970s, the company Litton introduced several new NMRG approaches based on combinations of alkali atoms and noble-gases [17], [26], [27].

The noble-gas nuclei were polarized via spin-exchange optical pumping with spin-polarized alkali atoms, which were also used as a magnetometer to sense noble-gas nuclear precession. They proposed using an alkali-incremental magnetometer, which was introduced in [28], [29], [30] and reviewed by Hartman [31], which allows for very sensitive magnetometry near zero magnetic field under the condition that $|B_0| < 1/|\gamma| \tau$ (the ground-state Hanle condition). τ is the alkali spin relaxation period. The method is also said to work when the condition $B_0 = n\omega/|\gamma|$ is satisfied, where n is an integer.

A bonus of performing in-cell magnetometry using an alkali magnetometer to sense the noble-gas magnetization is that the field generated by the noble-gas nuclei is magnified by orders of magnitude over what one would expect classically [32]. The enhancement arises from the hyperfine contact interaction through collisions [33], [34].

The Litton group also published work on cell fabrication, and reported an enhancement of the nuclear spin relaxation time by a factor of four by using rubidium hydride antirelaxation coatings on the inner cell walls [35], [36]. They also noticed that as they changed the cell temperature, the NMRG bias would drift until it reached a point where the drift would change sign. By operating at the "temperature turning point", the system was less sensitive to temperature fluctuations [37]. The Litton NMRG achieved a bias instability near 0.01 °/h and an ARW of 0.002 °/√h [38].

A ^{129}Xe NMRG developed at the University of Stuttgart published an ARW result of 1.7 °/√h [39]. The same group also demonstrated an enhancement of the ^{129}Xe signal size at relatively high fields by extending the regime of the ground-state Hanle condition to higher magnetic fields by using a strong light-shift laser to shift the effective magnetic field as seen by the Rb to near zero magnetic field [40].

V. Nuclear Quadrupolar Effects

One interesting and important systematic frequency shift in NMRGs arises from nuclear quadrupolar resonance (NQR) shifts [41]. NQR shifts arise from interactions between the atom's nuclear quadrupole moment and the electric-field gradient that is generated during collisions between the atoms and the cell walls, and is present for all nuclei that have nuclear quadrupole moments. All nuclei that have a nuclear spin of $I > ½$ have nuclear quadrupole moments, which includes ^{201}Hg and all $I \neq 0$ noble gases except for ^{3}He and ^{129}Xe. Because of its very long spin pump-up period, ^{3}He was not extensively studied for NMRGs. For all of the dual-isotope NMRGs that are presented in this review, at least one of the nuclear magnetic isotopes has had a nuclear quadrupole moment. The size of the shift depends on the angle between the cell's symmetry axis and the magnetic field.

NQR shifts were studied at length by the companies developing NMRGs for ^{83}Kr [42], ^{201}Hg [43], [44], and ^{131}Xe [45]. In these studies, the shifts caused decay and low-frequency beating of the NMRG signals, but the shifts were not large enough to be well resolved.

Happer's group demonstrated a ~100× enhancement in the size of the shifts by use of highly asymmetric cells [46], and presented a detailed microscopic theory of the interactions [47] which they compared to experiments [48]. The large NQR interactions in their system allowed them to perform detailed quantitative studies of the electric field gradients and the activation energies for surface adsorption.

Mehring's group also performed similar studies on ^{131}Xe [49] and ^{83}Kr [50], and they showed that the longer nuclear spin relaxation periods for ^{83}Kr allowed for higher spectral resolution of the NQR shifts. They also observed deviations from Berry's adiabatic geometric phase in the form of a nonlinear dependence of the measured NQR frequencies on the rotation rate in a highly asymmetric cell [51].

Our group at NIST has performed an NQR study on ^{131}Xe nuclei in a microfabricated cell of 1 mm^3 volume [52]. Four of the cell walls were silicon and two were pyrex. In our study, the strong electric field gradient (~30 GV/cm^2) was generated by anisotropy in the cell wall materials as opposed to the cell shape. We observed even larger NQR shifts than were seen in cells with asymmetric shapes [48], and were able to map the shifts in the regime where the NQR shifts are larger than the Larmor frequency.

VI. Comagnetometer

The Romalis group at Princeton has developed a novel version of an NMR gyroscope based on a potassium-^{3}He comagnetometer that demonstrated an ARW of 0.002 °/√h and a bias instability of 0.04 °/h [53]. They developed the comagnetometer to perform sensitive tests of physics beyond the standard model. They operated the potassium magnetometer in the spin-exchange relaxation free regime, in which relaxation from spin-exchange collisions is strongly suppressed [54]. The comagnetometer suppresses the sensitivity to magnetic fields, gradients and transients, light shifts, and spin-exchange shifts. A comagnetometer based on ^{21}Ne would probably exhibit improvement in stability by an order of magnitude resulting from its smaller gyromagnetic ratio (1/10 that of ^{3}He).

VII. NMRG Miniaturization

Research on NMRGs slowed after the early rush of activity when ring-laser gyroscopes (RLGs) with roughly the same size, weight, and power were achieving a value of 0.0005 °/√h for the ARW [55]. Because the ARW of an RLG is inversely proportional to the area enclosed by the laser beams, RLG performance diminishes for micro-scale devices. NMR gyroscopes have received renewed attention in recent years at least in part because of the advances made in chip-scale atomic clocks. These advances include MEMS vapor cells, instrumentation, and electronics that could be applied to high-performance chip-scale NMRGs. For reviews of chip-scale atomic clocks and magnetometers, see [56] and [57]. For some applications, NMR gyroscopes have the potential

advantage over micromachined spinning or vibratory gyroscopes in that they contain no moving parts.

Several patents on chip-scale NMRGs have emerged from Northrop Grumman in recent years [58], [59], [60], [61]. Reference [58] presents a scheme for using batch processing to develop a chip-scale atomic gyroscope. To enable low power consumption, the proposed device uses permanent magnets and low-power vertical-cavity surface emitting lasers. Designs are presented to allow for perpendicular pumping and probing which enable detection of Faraday rotation. Two of the patents pertain to cell fabrication techniques [59], [60], and one patent [61] presents a method of using three noble-gas isotopes to allow correction for NMR frequency shifts caused by the alkali polarization [62]. These shifts depend on cell temperature and laser power and can ultimately limit the bias stability.

Shkel's group at the University of California at Irvine has performed recent work on NMRGs specifically directed at developing microfabrication techniques. One of their key advances was the development of fabrication techniques to produce wafer-level arrays of glass blown spherical microcells [63], [64]. These cells allow optical access from nearly all directions and allow versatility in the pump/probe geometry. In collaboration with our group at NIST, these glass-blown cells were filled with Rb and buffer gases and their spectroscopic viability was demonstrated [65]. Also in collaboration with our group at NIST, Shkel's group developed a hybrid bulk micromachining and multilayer plasma-enhanced chemical vapor deposition process for depositing thin-film mirrors onto angled cell walls [66]. They solved the problem of thickness variation of the deposited reflectors caused by shadowing by depositing multiple shifted quarter-wave Bragg reflectors in series, and demonstrated less than 2 dB of return loss with circular polarization ellipticity maintained to ± 2° [67]. Like the micro glass-blown cells, these cells also allow for pumping and probing along different directions. Shkel's group has also performed work on thermal modeling related to NMRGs [68]. A summary of the components developed in Shkel's group as well as their integration can be found in [69].

The company Honeywell has also proposed an idea for a chip-scale NMRG [70]. Their physics package design is similar to the design for their chip-scale atomic clock [71], and they use the comagnetometer approach to sensing rotation that was developed by the Romalis group [53].

ACKNOWLEDGMENT

The author gratefully acknowledges J. Kitching, E. Hodby, T.C. Liebisch, and A. Shkel for stimulating discussions and collaborations. This work is sponsored by NIST, an agency of the U. S. government, and is not subject to copyright.

REFERENCES

[1] Products or companies named here are cited only in the interest of complete scientific description, and neither constitute nor imply endorsement by NIST or by the US government.

[2] F. A. Karwacki, "Nuclear Magnetic Resonance Gyro Development," Navigation: J. of the Institute of Navigation, vol. 27, pp. 72-8, 1980.

[3] K. F. Woodman, P. W. Franks, and M. D. Richards, "The Nuclear Magnetic Resonance Gyroscope: A Review," J. Navig., vol. 40, pp. 366-84, 1987.

[4] M. M. Kuritsky et al., "Inertial Navigation," Proc. IEEE, vol. 71, pp. 1156-76, 1983.

[5] K. Liu, "The Development of Micro-Gyroscope Technology," J. Micromech. Microeng., vol. 19, 113001, 2009.

[6] S. Xu, S. M. Rochester, V. V. Yaschuk, M. H. Donaldson, and D. Budker, "Construction and applications of an atomic magnetic gradiometer based on nonlinear magneto-optical rotation," Rev. Sci. Instrum., vol. 77, 083106, 2006.

[7] E. A. Donley, E. Hodby, L. Hollberg, and J. Kitching, "Demonstration of high-performance compact magnetic shields for chip-scale atomic devices," Rev. Sci. Instrum., vol. 78, 083102, 2007.

[8] J. H. Simpson, J. T. Fraser, and I. A. Greenwood, "An Optically Pumped Nuclear Magnetic Resonance Gyroscope," IEEE Trans. Aerosp. Support, vol. 1, pp. 1107-10, 1963.

[9] B. D. Leete, "Apparatus for Measuring Angular Motion," U. S. Patent No. 2,720,625, 1955.

[10] A. Hansen, "Method and Apparatus for Measuring Angular Motion," U. S. Patent No. 2,841,760, 1958.

[11] S. M. Forman and M. J. Minneman, "A Magnetic Induction Gyroscope," IEEE. Trans. Military Electronics, vol. 7, pp. 40-4, 1963.

[12] A. Kastler, "Quelques Suggestions Concernant la Production Optique et la Détection Optique Dune Inégalité de Population des Niveaux de Quantification Spatiale des Atomes - Application a l'experience de Stern et Gerlach et a la Résonance Magnétique," J. Phys. Radium, vol. 11, pp. 225, 1950.

[13] W. Happer, "Optical Pumping," Rev. Mod. Phys., vol. 44, pp. 169-249, 1972.

[14] J. T. Fraser, "Optically Pumped Magnetic Resonance Gyroscope and Direction Sensor, U. S. Patent No. 3,103,621, 1963.

[15] J. M. Andres, "Optically Pumped Gyromagnetic Apparatus," U. S. Patent No. 3,204,683, 1965.

[16] M. A. Bouchiat, T. R. Carver, and C. M. Varnum, "Nuclear Polarization in He^3 Gas Induced by Optical Pumping and Dipolar Exchange," Phys. Rev. Lett., vol. 5, pp. 373-5, 1960.

[17] E. Kanegsberg, "A Nuclear Magnetic Resonance (NMR) Gyro with Optical Magnetometer Detection," SPIE Laser Inertial Rot. Sens., vol. 157, pp. 73-80, 1978.

[18] T. G. Walker and W. Happer, "Spin-Exchange Optical Pumping of Noble-Gas Nuclei," Rev. Mod. Phys., vol. 69, pp. 629-42, 1997.

[19] H. G. Dehmelt, "Modulation of a Light Beam by Precessing Absorbing Atoms," Phys. Rev., vol. 105, pp. 1924-25, 1957.

[20] D. Budker, W. Gawlik, D. F. Kimball, S. M. Rochester, V. V. Yashchuk, and A. Weis, "Resonant nonlinear magneto-optical effects in atoms," Rev. Mod. Phys., vol. 74, pp. 1153-1201, 2002.

[21] J. H. Simpson, "Nuclear Gyroscopes," Astronautics & Aeronautics, vol. 2, pp. 42-8, 1964.

[22] D. S. Bayley, I. A. Greenwood, and J. H. Simpson, "Optically Pumped Nuclear Magnetic Resonance Gyroscope," U. S. Patent No. 3,778,700, 1973.

[23] I. A. Greenwood, "Nuclear Gyroscope with Unequal Fields," U. S. Patent No. 4,147,974, 1979.

[24] I. A. Greenwood and J. H. Simpson, " Fundamental Noise Limitations in Magnetic Resonance Gyroscopes," Proc. IEEE 1977 National Aerospace and Electronics Converence, NAECON, pp. 1246-50, 1977.

[25] F. A. Karwacki and J. Griffin, "Nuclear Magnetic Resonance Gyroscope," U. S. Patent No. 4,509,014, 1985.

[26] B. C. Grover, E. Kanegsberg, J. G. Mark, and R. L. Meyer, "Nuclear Magnetic Resonance Gyro," U. S. Patent No. 4,157,495, 1979.

[27] B. C. Grover, "Nuclear Magnetic Resonance Gyroscope," U. S. Patent No. 4,430,616, 1984.

[28] J. Dupont-Roc, S. Haroche, and C. Cohen-Tannoudji, "Detection of Very Weak Magnetic Fields (10^{-9} Gauss) by ^{87}Rb Zero-Field Level Crossing Resonances," Phys. Lett., vol. 28A, pp. 638-9, 1969.

[29] C. Cohen-Tannoudji, J. Dupont-Roc, S. Haroche, and F. Laloë, "Diverses Rèsonances de Croisement de Niveaux sure des Atomes Pompès Optiquement en Champ Nul I. Thèorie," Rev. de Phys. Appliq., vol. 5, pp. 95-101, 1970.

[30] C. Cohen-Tannoudji, J. Dupont-Roc, S. Haroche, and F. Laloë, "Detection of the Static Magnetic Field Produced by the Oriented Nuclei of Optically Pumped ^{3}He Gas," Phys. Rev. Lett., vol. 22, pp. 758-60, 1969.

[31] F. Hartman, "Resonance Magnetometers," IEEE. Trans. Magn., vol. MAG-8, pp. 66-75, 1972.

[32] B. C. Grover, "Noble-Gas NMR Detection through Noble-Gas-Rubidium Hyperfine Contact Interaction," Phys. Rev. Lett., vol. 40, pp. 391-2, 1978.

[33] R. M. Herman, "Theory of Spin Exchange between Optically Pumped Rb and Foreign Gas Nuclei," Phys. Rev., vol. 137, pp. A1062-65, 1965.

[34] R. L. Gamblin and T. R. Carver, "Polarization and Relaxation Processes in He^3 Gas," Phys. Rev., vol. 138, pp. A946-60, 1965.

[35] T. M. Kwon and C. H. Volk, "Magnetic Resonance Cell," U. S. Patent No. 4,446,428, 1984.

[36] T. M. Kwon and W. P. Debley, "Magnetic Resonance Cell and Method for its Fabrication," U. S. Patent No. 4,450,407, 1984.

[37] T. M. Kwon, "Nuclear Magnetic Resonance Cell Having Improved Temperature Sensitivity and Method for Manufacturing Same," U. S. Patent No. 4,461,996, 1984.

[38] L. K. Lam, E. Phillips, E. Kanegsberg, and G. W. Kamin, "Application of CW Single-Mode GaAlAs Lasers to Rb-Xe NMR Gyroscopes," Proc. SPIE, vol. 412, pp. 272-6, 1983.

[39] P. Härle, G. Wäckerle, and M. Mehring, " A Nuclear-Spin Based Rotation Sensor Using Optical Polarization and Detection Methods," Appl. Magn. Reson., vol. 5, pp. 207-20, 1993.

[40] S. Appelt, H. Langen, G. Wäckerle, and M. Mehring, "Separation of the Magnetic Quantization Axes by Lightshift Interaction in a Rb/Xe Gas Mixture," Opt. Commun., vol. 96, pp. 45-51, 1993.

[41] C. Cohen Tannoudji, "Relaxation Quadrupolaire de l'Isotope ^{201}Hg sur des Parois de Quartz," J. Phys., vol. 24, pp. 653-60, 1963.

[42] C. H. Volk, J. G. Mark, and B. C. Grover, "Spin Dephasing of ^{83}Kr," Phys. Rev. A, vol. 20, pp. 2381-8, 1979.

[43] P. A. Heimann, " Quadrupole Perturbation Effects upon the ^{201}Hg Magnetic Resonance. I. Effects upon Free Precession of the Nuclear Spins," Phys. Rev. A, vol. 23, pp. 1204-8, 1981.

[44] P. A. Heimann, I. A. Greenwood, and J. H. Simpson, "Quadrupole Perturbation Effects upon the ^{201}Hg Magnetic Resonance. II. Relaxation due to an Anisotropic Perturbation," Phys. Rev. A, vol. 23, pp. 1209-14, 1981.

[45] T. M. Kwon, J. G. Mark, and C. H. Volk, "Quadrupole Nuclear Spin Relaxation of ^{131}Xe in the Presence of Rubidium Vapor," Phys. Rev. A, vol. 24, pp. 1894-1903, 1981.

[46] Z. Wu, W. Happer, and J. M. Daniels, "Coherent Nuclear-Spin Interactions of Adsorbed ^{131}Xe Gas with Surfaces," Phys. Rev. Lett., vol. 59, pp. 1480-3, 1987.

[47] Z. Wu, S. Schaefer, G. D. Cates, and W. Happer, "Coherent Interactions of the Polarized Nuclear Spins of Gaseous Atoms with the Container Walls," Phys. Rev. A, vol. 37, pp. 1161-75, 1988.

[48] Z. Wu, W. Happer, M. Kitano, and J. Daniels, "Experimental Studies of Wall Interactions of Adsorbed Spin-Polarized ^{131}Xe Nuclei," Phys. Rev. A, vol. 42, pp. 2774-84, 1990.

[49] R. Butscher, G. Wäckerle, and M. Mehring, "Nuclear Quadrupole Interaction of Highly Polarized Gas Phase ^{131}Xe with a Glass Surface," J. Chem. Phys., vol. 100, pages 6923-33, 1994.

[50] R. Butscher, G. Wäckerle, and M. Mehring, "Nuclear Quadrupole Surface Interaction of Gas Phase 83Kr: Comparison with ^{131}Xe," Chem. Phys. Lett., vol. 249, pp. 444-50, 1996.

[51] S. Appelt, G. Wäckerle, and M. Mehring, "Deviation from Berry's Adiabatic Geometric Phase in a ^{131}Xe Nuclear Gyroscope," Phys. Rev. Lett., vol. 72, pp. 3921-4, 1994.

[52] E. A. Donley, J. L. Long, T. C. Liebisch, E. R. Hodby, T. A. Fisher, and J. Kitching, "Nuclear Quadrupole Resoances in Compact Vapor Cells, The Crossover Between the NMR and the nuclear Quadrupole resonance Interaction Regimes," Phys. Rev. A, vol. 79, 013420, 2009.

[53] T. W. Kornack, R. K. Ghosh, and M. V. Romalis, "Nuclear Spin Gyroscope Based on an Atomic Comagnetometer," Phys. Rev. Lett., vol. 95, 230801, 2005.

[54] I. K. Kominis, T. W. Kornack, J. C. Allred, and M. V. Romalis, "A subfemtotesla multichannel atomic magnetometer," Nature, vol. 422, pp. 596-599, 2003.

[55] W. W. Chow, J. Gea-Banacioche, L.M. Pedrotti, V. E. Sanders, W. Schleich, and M. O. Scully, "The Ring Laser Gyro," Rev. Mod. Phys., vol. 57, pp. 61-104, 1985.

[56] S. Knappe, "MEMS Atomic Clocks," Comprehensive Microsystems, vol. 3, pp. 571-612, 2007.

[57] J. Kitching et al., "Chip-scale Atomic Devices: Precision Atomic Instruments Based on MEMS," Proc. 2008 Symp. Freq. Stds. Metrology, pages 445-53, 2008.

[58] H. C. Abbink, E. Kanegsberg, and R. A. Patterson, "NMR Gyroscope," U. S. Patent No. 7,239,135 B2, 2007.

[59] H. C. Abbink, E. Kanegsberg, K. D. Marino, and C. H. Volk, "Micro-Cell for NMR Gyroscope," U.S. Patent No. 7,292,031 B2, 2007.

[60] H. C. Abbink, W. P. Debley, C. E. Goesling, D. K Sakaida, and R. E. Stewart, "Middle Layer of Die Structure that Comprises a Cavity that Holds an Alkali Metal," U. S. Patent No. 7,292,111 B2, 2007.

[61] E. Kanegsberg, "Nuclear Magnetic Resonance Gyroscope," U. S. Patent No. 7,282,910 B1, 2007.

[62] N. R. Newbury et al., "Polarization-Dependent Frequency Shifts from Rb-^{3}He Collisions," Phys. Rev. A, vol. 48, pp. 558-68, 1993.

[63] E. J. Eklund and A. M. Shkel, "Glass Blowing on a Wafer Level," J. Microelectromech. Syst., vol. 16, pp. 232-239, 2007.

[64] E. J. Eklund and A. M. Shkel, "Method and Apparatus for Wafer-Level Micro-Glass-Blowing," U. S. Patent No. 7,694,531 B2, 2010.

[65] E. J. Eklund, A. M. Shkel, S. Knappe, E. Donley, and J. Kitching, "Glass-Blown Spherical Microcells for Chip-Scale Atomic Devices," Sens. Actuators, A., vol. 143, pp. 175-180, 2008.

[66] M. A. Perez, U. Nguyen, S. Knappe, E. A. Donley, J. Kitching, and A. Shkel, "Rb Vapor Cell with Integrated Bragg Reflectors for Compact Atomic MEMS," Sens. Actuators, A., vol. 154, pp. 295-303, 2009.

[67] M. A. Perez, J. Kitching, and A. Shkel, "Design Demonstration of PECVD Multilayer Dielectric Mirrors Optimized for Micromachined Cavity Angled Sidewalls," Sens. Actuators, A., vol. 155, pp. 23-32, 2009.

[68] M. Salleras, E. J. Eklund, I. P. Prikhodko, and A. M. Shkel, "Predictive Thermal Model for Indirect Temperature Measurement Inside Atomic Cell of Nuclear Magnetic Resonance Gyroscope," Proc. Transducers 2009, pp. 304-307, 2009.

[69] E. J. Eklund, "Microgyroscope Based on Spin-Polarized Nuclei," Ph.D. Thesis, University of California at Irvine, 2008.

[70] L. M. Lust and D. W. Youngner, "Chip Scale Atomic Gyroscope," U. S. Patent No. 7,359,059 B2, 2008.

[71] D. W. Youngner et al., "A Manufacturable Chip-Scale Atomic Clock," Transducers & Eurosensors '07, Lyon, France, pp. 39-44, 2007.